Geminate recombination in protontransfer reactions. II. Comparison of diffusional and kinetic schemes

Noam Agmon, Ehud Pines, and Dan Huppert

Citation: J. Chem. Phys. **88**, 5631 (1988); doi: 10.1063/1.454573
View online: http://dx.doi.org/10.1063/1.454573
View Table of Contents: http://jcp.aip.org/resource/1/JCPSA6/v88/i9
Published by the American Institute of Physics.

Geminate recombination in proton-transfer reactions. II. Comparison of diffusional and kinetic schemes

Noam Agmon[a)]
Department of Physical Chemistry, The Hebrew University, Jerusalem 91904, Israel

Ehud Pines and Dan Huppert
School of Chemistry, Sackler School of Exact Sciences, Tel-Aviv University, Tel-Aviv 69978, Israel

(Received 30 July 1987; accepted 20 August 1987)

The diffusional and kinetic approaches are compared for geminate dissociation–recombination reactions. When steady-state rate coefficients to and from a distance defined as a "complex cage" are evaluated from the diffusion equation, one obtains encouraging agreement between the transient analytic solution of the rate equations and the exact numerical solution for diffusion with backreaction over a finite time regime. However, the rate equations cannot accurately describe the decay of the dissociating molecule for very long times, since as we prove below, the asymptotic decay according to the diffusional scheme is $t^{-3/2}$, while for the rate equations it is exponential. New experiments, over an extended time regime confirm these conclusions.

I. INTRODUCTION

The Debye–Smoluchowski diffusion equation (DSE)[1,2] has been used for a long time for describing chemical reactions in solution.[1–6] A prominent example is geminate recombination: If it is very fast one uses a Smoluchowski (absorbing) boundary condition[1,2] and the reaction is called "diffusion controlled." If association is not extremely fast, one uses the so-called "radiation" boundary condition.[3] This accounts for cases where not every encounter leads to reaction, but still completely neglects the reverse, dissociation reaction. More complex boundary conditions which take backreaction into account have appeared in the literature,[7] but only recently[8] has their applicability been demonstrated for explaining experimental data of picosecond geminate dissociation–recombination of an excited-state acid.[9]

Although it was possible[8] to describe transient kinetics by solving the DSE, which is a partial-differential equation, the customary approach in chemical kinetics[10] is to solve ordinary differential equations namely, the rate equations. For proton-transfer and other reactions one often writes a kinetic scheme[4] of the type

$$\mathrm{AB} \underset{k_2}{\overset{k_1}{\rightleftarrows}} \mathrm{A}\cdots\mathrm{B} \underset{k_D}{\overset{k_{-D}}{\rightleftarrows}} \mathrm{A}+\mathrm{B}. \tag{1}$$

The molecule AB first dissociates into a "complex" A···B, which eventually separates into A and B. Here k_1 and k_2 are dissociation and recombination rate constants, while k_D and k_{-D} are diffusional rate parameters.

Historically,[4] predictions from Eq. (1) were compared with steady-state results. In the present study we investigate the temporal behavior of this scheme. Two major questions are raised: (a) How well does the (bi-exponential) transient solution for the kinetic scheme (1) compare with picosecond experiments on excited-state proton dissociation? (b) How should one define the complex cage so that optimal agreement is obtained?

Our work is divided into two major part: In Secs. II and III we modify a previously proposed procedure[5] for evaluating the rate coefficients in Eq. (1): Rather than taking the complex separation equal to the "contact distance" a, where the boundary conditions for the DSE are imposed, we assume that the complex cage has a much larger spatial extent $R_{cc} > a$. This is in line with discussions[4,10–13] of the "Coulomb cage" in ionic reactions, where R_{cc} is of the order of the Debye radius R_D, which scales the Coulomb attractive forces R_D/r^2. The situation is depicted schematically in Fig. 1. By adjusting R_{cc}, we find good agreement between the diffusional and kinetic schemes over finite time regimes

Other work on the cage effect[14,15] views it as arising mainly from the microscopic structure of the solvent, which introduces additional barriers along the diffusional path. This solvent cage is different than the Coulomb cage mentioned here: Because the potential is completely monotonic in r, the "cage" in this work has nothing to do with the discrete structure of the solvent.

The second part of this work, Secs. IV and V, shows that the rate equations cannot fit experiment over an extended time regime. In Sec. IV we prove that the asymptotic decay of the population of the dissociating molecules approaches a $t^{-3/2}$ behavior at long times. A kinetic scheme with a finite number of consecutive states is a superposition of exponentials. It can never rigorously approach a power law. In Sec. V we extend our previous experiments[8(a)] to longer times. These results indeed support the power-law asymptotic behavior.

II. EVALUATION OF DIFFUSIONAL RATE COEFFICIENTS

A. The Deby–Smoluchowski equation with backreaction

In the continuous diffusion approach[1–6] one describes the chemical reaction (1) by a spherically symmetric diffusion equation (DSE) in three dimensions:

[a)] Address until August 1988: NIH, DCRT, Bld. 12A, Rm. 2007, Bethesda, MD 20892.

 0021-9606/88/095631-08$02.10

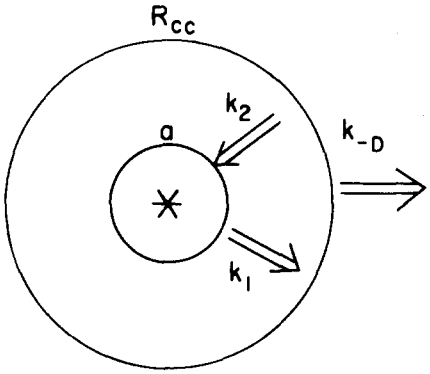

FIG. 1. A schematic representation of the suggested procedure for calculating diffusional rate parameters for scheme (1). The boundary condition for the DSE (2) is imposed at the inner sphere, $r=a$ (the "contact distance"). The geminate pair is called a "complex" when their separation is in between the two spheres, $a \leqslant r \leqslant R_{cc}$. The rate coefficients in scheme (1) are calculated from the steady-state diffusional fluxes to and from the "complex cage" separation, R_{cc}, see Sec. II C below.

$$\frac{\partial p(r,t)}{\partial t} = -(4\pi r^2)^{-1}\frac{\partial J}{\partial r}$$

$$= r^{-2}\frac{\partial}{\partial r} Dr^2 e^{-V}\frac{\partial}{\partial r} e^{V} p, \quad r \geqslant a . \tag{2}$$

Here $p(r,t)$ is a probability density function for the geminate pair A,B to be separated by a distance r at time t, D is a diffusion coefficient (assumed here a constant), and $V(r)$ is a potential function divided by $k_B T$. J is the diffusional flux.

The boundary conditions at $r=a$ are those of backreaction[7]

$$J(a,t) = \kappa_d [1 - Q(t)] - \kappa_r 4\pi a^2 p(a,t) , \tag{3}$$

where

$$Q(t) \equiv 4\pi \int_a^\infty p(r,t) r^2 \, dr \tag{4}$$

is the survival probability for the dissociated geminate pair, and κ_d and κ_r are the "intrinsic" dissociation and recombination rate constants at the contact distance a. The more customary[3] radiation boundary condition is a special case with $\kappa_d = 0$. We assume that initially one has only AB so that

$$p(r,0) = 0 . \tag{5}$$

We have previously[8] demonstrated the solution of Eqs. (2)–(5) and its comparison to experiment. We now wish to compare it to that of the kinetic scheme (1), namely to compare the survival probability of AB with $1 - Q(t)$ and the survival probability of the complex A···B with

$$Q_{cc}(t) \equiv 4\pi \int_a^{R_{cc}} p(r,t) r^2 \, dr , \tag{6}$$

R_{cc} is the radius of the complex cage (the "Coulomb cage" for ions).

B. The rate equations

For the geminate stage one can ignore the homogenous recombination in Eq. (1) and hence the term with k_D. The kinetic equations then read

$$\frac{d[\mathrm{AB}]}{dt} = -k_1[\mathrm{AB}] + k_2[\mathrm{A}\cdots\mathrm{B}] , \tag{7a}$$

$$\frac{d[\mathrm{A}\cdots\mathrm{B}]}{dt} = k_1[\mathrm{AB}] - (k_2 + k_{-D})[\mathrm{A}\cdots\mathrm{B}] . \tag{7b}$$

The initial conditions are

$$[\mathrm{AB}](t=0) = 1, \quad [A\cdots B](t=0) = 0 . \tag{8}$$

These kinetic equations are solvable analytically exactly (no steady-state approximation needed), as a set of first order linear differential equations with constant coefficients.[4] The two (negative) eigenvalues, λ_+ and λ_-, are determined by setting the determinant of coefficients to zero:

$$2\lambda_\pm = -(k_1 + k_2 + k_{-D}) \pm \Delta , \tag{9a}$$

$$\Delta \equiv [(k_1 + k_2 + k_{-D})^2 - 4k_1 k_{-D}]^{1/2} . \tag{9b}$$

For the given initial conditions the solution reads

$$[\mathrm{AB}](t) = [(k_1 + \lambda_+)\exp(\lambda_- t) - (k_1 + \lambda_-)\exp(\lambda_+ t)]/\Delta , \tag{10a}$$

$$[\mathrm{A}\cdots\mathrm{B}](t) = k_1[\exp(\lambda_+ t) - \exp(\lambda_- t)]/\Delta . \tag{10b}$$

C. Calculating the rate coefficients

The steady-state rate coefficients in Eq. (7) can be calculated from the steady-state condition for Eq. (2),

$$J^{ss}(r) \equiv -4\pi D r^2 \exp[-V(r)] \times \frac{d}{dr}\exp[V(r)] p^{ss}(r) = \text{const} , \tag{2'}$$

with the appropriate boundary conditions. There is no need to find first[5,6] the steady-state solution, $p^{ss}(r)$: A rate coefficient k can be calculated by direct integration of Eq. (2'), with $J^{ss} = k$ in the dissociation direction and $J^{ss} = -k$ for reactions in the association direction (J is positive for increasing r). We assume that $V(r) \to 0$ as $r \to \infty$. We omit the superscript *ss* for brevity. All bimolecular rates below are per molecule. To obtain the bimolecular rate coefficients in the conventional units of $\mathrm{M}^{-1}\,\mathrm{s}^{-1}$, the expressions below should be evaluated in cgs units and multiplied by $\mathrm{N_A}/1000$, where $\mathrm{N_A}$ is Avogadro's number. The solution is as follows:

(i) Diffusion rate from infinity to complex, k_D. Although we do not need this rate constant, we give it for completeness. The boundary conditions are

$$p(R_{cc}) = 0, \quad p(\infty) = 1 . \tag{11a}$$

Integration of Eq. (2') from R_{cc} to ∞ gives

$$4\pi D\, k_D^{-1} = \int_{R_{cc}}^\infty \exp[V(r)] r^{-2} \, dr . \tag{12a}$$

(ii) Reverse diffusion rate from complex to infinity, k_{-D}. Boundary conditions are

$$p(R_{cc}) = v_{cc}^{-1}, \quad p(\infty) = 0 , \tag{11b}$$

where

$$v_{cc} = 4\pi(R_{cc}^3 - a^3)/3 \tag{13}$$

is the volume of the spherical shell extending from $r=a$ to $r=R_{cc}$ and defining the complex cage. (The correction for

the excluded volume, $4\pi a^3/3$, would be negligible for large R_{cc}.) Integration of Eq. (2') yields

$$4\pi D\,(k_{-D}\,v_{cc})^{-1}\exp[V(R_{cc})] = \int_{R_{cc}}^{\infty}\exp[V(r)]r^{-2}\,dr\,.$$

(iii) Geminate recombination rate of complex, k_2. Boundary conditions are

$$J(a) = -4\pi a^2\kappa_r p(a),\quad p(R_{cc}) = v_{cc}^{-1}\,. \tag{11c}$$

Integration gives

$$4\pi D\exp[V(R_{cc})]\,(k_2 v_{cc})^{-1} = \int_a^{R_{cc}}\exp[V(r)]r^{-2}\,dr + D\exp[V(a)]/(a^2\kappa_r)\,, \tag{12c}$$

k_2 itself can be decomposed into more fundamental steps[15] (see Appendix A).

(iv) Dissociation rate constant k_1. Boundary conditions are

$$J(a) = \kappa_d,\quad p(R_{cc}) = 0\,. \tag{11d}$$

Note that κ_d is not multiplied here by $1 - Q_{cc}$ as in Eq. (3), since a steady-state source of AB molecules is postulated. The constant-flux solution must therefore be equal to the flux at the boundary, hence

$$k_1 = \kappa_d\,. \tag{12d}$$

In the special case of free diffusion, $V = 0$, Eqs. (12a)–(12c) become

$$k_D = 4\pi D R_{cc}\,, \tag{14a}$$

$$k_{-D} = 3DR_{cc}\,[R_{cc}^3 - a^3]^{-1}\,, \tag{14b}$$

$$k_2 = 3D\,[R_{cc}^3 - a^3]^{-1}\times[a^{-1} - R_{cc}^{-1} + D/(a^2\kappa_r)]^{-1}\,. \tag{14c}$$

For a Coulomb potential, $V(r) = -R_D/r$, the expressions for the rate coefficients become

$$k_D = 4\pi D R_D\,[1 - \exp(-R_D/R_{cc})]^{-1}\,, \tag{15a}$$

$$k_{-D} = 3D\,R_D\,[R_{cc}^3 - a^3]^{-1}[\exp(R_D/R_{cc}) - 1]^{-1}\,, \tag{15b}$$

$$k_2 = \frac{3DR_D}{R_{cc}^3 - a^3}\exp(-R_D/R_{cc})\Big[\exp(-R_D/R_{cc}) - \exp(-R_D/a) + \frac{DR_D}{a^2\kappa_r}\exp(-R_D/a)\Big]^{-1}\,. \tag{15c}$$

Note that only the two rate coefficients out of the complex, k_{-D} and k_2, depend on R_{cc}.

D. Steady-state rates

Finally, we discuss the steady-state *on*- and *off*-rate coefficients for the scheme (1), namely the overall steady-state association and dissociation fluxes, respectively. The *on* rate, which is given by[4,5]

$$k_{on} = k_D\,k_2/(k_2 + k_{-D}) \tag{16}$$

is also independent of R_{cc}, since by Eqs. (12a) and (12c),

$$\frac{1}{k_{on}} = \frac{1}{k_D} + \frac{\exp[V(R_{cc})]}{v_{cc}\,k_2} = (4\pi D)^{-1}\Big[\int_a^{\infty}\exp[V(r)]r^{-2}\,dr + \frac{D\exp[V(a)]}{a^2\kappa_r}\Big]\,. \tag{17}$$

This result is similar to Eq. (12c) with R_{cc} replaced by ∞. In the special case of an attractive Coulomb potential it reads

$$k_{on} = 4\pi D R_D/[1 + (D\,R_D/a^2\kappa_r - 1)\exp(-R_D/a)]\,. \tag{17'}$$

Because it is independent of R_{cc}, it does not uniquely determine[5] the rate coefficients k_2 and k_{-D}, which do depend on R_{cc}. These have to be determined from a comparison with transient results. Appendix B shows how the reaction probability[17] from $r = R_{cc}$ is related to the abovementioned rate coefficients.

The *off* rate, which is the area under the decay curve, does depend on R_{cc}. It may be defined from Eq. (10a) as

$$k_{off}^{-1} \equiv \int_0^{\infty}[AB](t)dt = \frac{k_1 + \lambda_-}{\lambda_+\Delta} - \frac{k_1 + \lambda_+}{\lambda_-\Delta} = \frac{k_2 + k_{-D}}{k_1 k_{-D}}\,. \tag{18}$$

the last equality follows from Eq. (9a), and Δ is given by Eq. (9b).

When $[AB](t)$ is the approximation to the exact transient solution of the DSE obtained by optimizing R_{cc} in Eq. (10a), Eq. (18) gives only an approximate value for k_{off}. However, the exact steady-state solution of the DSE is easily obtained by evaluating k_2 and k_{-D} in Eq. (18) with $R_{cc} = a$ (the volume factor v_{cc} cancels). The reason is that under steady-state conditions the distribution for $r \geqslant a$ is stationary, and there is no need to postulate different constant fluxes for the regions of $r < R_{cc}$ and $r > R_{cc}$. For an attractive Coulomb potential the *off* rate is therefore given by

$$k_{off} = \kappa_d/\{1 + [\exp(R_D/a) - 1]a^2\kappa_r/DR_D\}\,. \tag{18'}$$

From the above, the dissociation equilibrium constant at infinite dilution can be obtained as

$$K_\infty = k_{off}/k_{on} = \frac{k_1\,k_{-D}(a)}{k_2(a)k_D(a)} = \kappa_d/\{4\pi a^2\kappa_r\exp[-V(a)]\}\,. \tag{19}$$

For ions, this is an accurate version of the Fuoss relation[12] for backreaction boundary conditions. A different derivation is given in subsequent work.[8(b)] It is customary to denote the excited-state dissociation constant by K^*.

III. COMPARISON ON A LINEAR SCALE

We demonstrate the above results for the measured[8(a)] photodissociation of hydroxypyrene-trisulfonate (HPTS), which we designate by ROH*. In Fig. 2 the bold lines are numerical solution[8(a)] to Eqs. (2)–(5), $1 - Q(t)$, which fit the HPTS data at room temperature. The dashed curves are the solution of Eqs. (9) and (10) to the kinetic scheme (1). The kinetic parameters k_{-D} and k_2 were calculated as in the

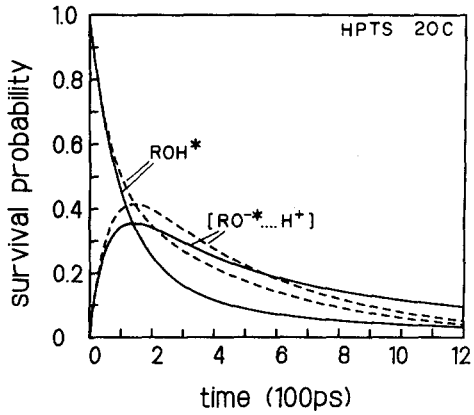

FIG. 2. Comparison of the exact numerical solution for diffusion with back-reaction [Eq. (2), bold curves] for the photochemical dissociation of HPTS, with the analytic solution of the kinetic scheme [Eq. (10), dashed curves]. The parameters in Eqs. (2), (3) are: $D = 930$ Å^2/ns, $a = 6.5$ Å, $R_D = 28.3$ Å, $\kappa_r = 12$ Å/ns, and $\kappa_d = 9.2$ ns^{-1}. The rate coefficients in the kinetic scheme (1) were evaluated as in Ref. 5: Eq. (15) was used with $R_{cc} = a$ and no excluded volume in Eq. (13). The values for the rate coefficients are: $k_{-D} = 3.7$ ns^{-1}, $k_2 = 5.5$ ns^{-1}, and $k_1 = \kappa_d = 9.2$ ns^{-1}. The eigenvalues, Eq. (9), are: $\lambda_+ = -2.10$ ns^{-1} and $\lambda_- = -16.4$ ns^{-1}. The amplitude of the slow component λ_+ is $-(k_1+\lambda_-)/\Delta = 0.506$. The transient concentration of the complex $RO^{-*} \cdots H^+$ is compared with Q_{cc}, Eq. (6), with $R_{cc} = R_D/2 = 14.1$ Å.

literature[5] namely, with $R_{cc} = a = 6.5$ Å in Eq. (15) but no excluded volume in Eq. (13). A poor agreement between $1 - Q$ and the temporal decay of [AB] is observed. The transient increase and decay of the intermediate A···B is compares with Q_{cc}, Eq. (6), with R_{cc} set arbitrarily to $R_D/2$.

Figure 3 shows that a much better agreement between the two schemes is obtained when Eq. (15) is used for the rate coefficients. The best value of R_{cc} is 27 Å, which is comparable with $R_D = 28.3$ Å, and much larger than $a = 6.5$ Å. Varying R_{cc} by a few angstroms affects only slightly the quality of agreement shown. The values that appear in the literature for this reaction are: $R_{cc} = 33$ Å[13] or $r_0 = 35$ Å[9] (r_0 in Ref. 9 should probably be interpreted as the complex cage radius). When compared with Fig. 2, this is admittedly a one-parameter (R_{cc}) fit to the numerical calculation. Unlike Fig. 2, however, the same value of $R_{cc} = 27$ Å is used in Eq. (6) for a comparison with [A···B]. A very similar value ($R_{cc} = 26$ Å) fits the results[8(a)] for HPTS in D_2O at 18 °C.

The present analysis is not limited to a Coulomb potential: Fig. 4 shows a comparison with the exact calculation for free diffusion, $R_D = 0$, where Eq. (14) was used for evaluating the rate coefficients, together with the value of $R_{cc} \approx 2a$. This value was chosen as the distance from which recombination and dissociation fluxes are equal, in analogy to the determination of dividing surfaces on gas-phase potential-energy surfaces.[16]

The values of the best parameters in Fig. 3 can be used to evaluate the observed *on* and *off* rates. As discussed above, the *on* rate is independent of R_{cc}. Equation (17) gives $k_{on} = 1.2\times10^{11}$ M^{-1} s^{-1}, as compared with $k_D = 2.1\times10^{11}$ M^{-1} s^{-1}, evaluated form Eq. (15a).

The *off*-rate constant, Eq. (18), does depend on R_{cc}. Using the parameters of Fig. 3 we find that $k_{off} = 5.6\times10^9$ s^{-1}. This is larger than the exact value of 3.9×10^9 s^{-1} obtained from Eq. (18'). The reason is that Eq. (10a), which decays exponentially, when adjusted to fit the transient results at short times, underestimates the long-time tail which obeys a power law (see below). Hence the kinetic scheme (1) is incapable of fitting simultaneously both the transient decay profile and its area, namely the steady-state dissociation rate coefficient k_{off}.

IV. ASYMPTOTIC BEHAVIOR

We have demonstrated above, that the solution (4) of the diffusion equation and that of the kinetic scheme, Eq. (10a), behave similarly on a linear scale. In order to detect substantial differences between the two approaches, one must consider their asymptotic behavior. The solution of the set of ordinary differential equations (7), for any finite number of consecutive steps, is an eigenvalue problem. Its

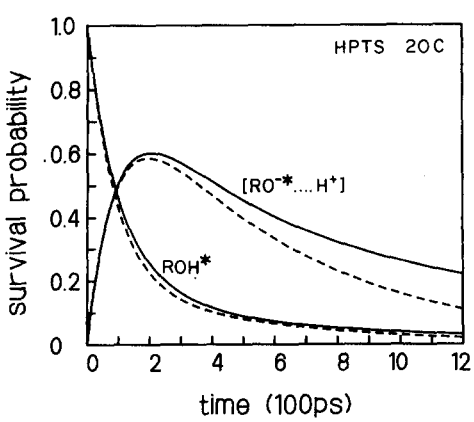

FIG. 3. Same as Fig. 2, but with rate coefficients evaluated from Eq. (15) with $R_{cc} = 27$ Å. This gives: $k_{-D} = 2.20$ ns^{-1}, $k_2 = 1.42$ ns^{-1}, and k_1 as before. The eigenvalues, Eq. (9), are: $\lambda_+ = -1.84$ ns^{-1} and $\lambda_- = -10.97$ ns^{-1}. The amplitude of the slow component λ_+ is $-(k_1+\lambda_-)/\Delta = 0.194$.

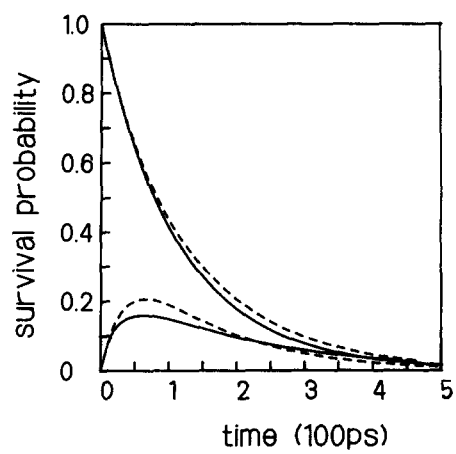

FIG. 4. Same as Fig. 3 for free diffusion, $R_D = 0$, with $R_{cc} = 12$ Å. This gives $k_{-D} = 21.77$ ns^{-1}, $k_2 = 0.745$ ns^{-1}, and k_1 as before. The eigenvalues are $\lambda_+ = 8.70$ ns^{-1} and $\lambda_- = 23.01$ ns^{-1}. The amplitude of the slow component is now 0.965.

asymptotic behavior is always exponential. We derive below the asymptotic behavior of $1-Q(t)$ for diffusion with backreaction, which is a power law. In order to check our derivation, we calculate in Appendix C the asymptotic behavior for free diffusion in one dimension, where the solution for backreaction can be obtained analytically.

The derivation of the asymptotic behavior for the survival probability in Eqs. (2) and (3) is based on the observation[8(c)] that at long times the probability distribution $p(r,t)$ approaches $p^r(r,t|a)$, which is obtained by replacing the backreaction boundary condition (3) by a reflecting boundary condition, $J(a,t)=0$, and starting from an initial delta function at $r=a$. The physical reason for this is clear. Introducing recombination and dissociation into the latter problem is equivalent to a time delay determined by the intrinsic rate constants κ_r and κ_d. As $t\to\infty$ this delay becomes negligible.

Based on the above logic, one finds from Eq. (3) that the asymptotic behavior for the survival probability

$$1-Q(t)\sim[4\pi a^2\kappa_r/\kappa_d]p^r(a,t|a) \tag{20}$$

is determined from the asymptotic behavior of the probability density function at the reflective boundary.

Let us consider first the case of free diffusion, $V(r)=0$. The solution for a reflective boundary condition, $\partial p/\partial r=0$ at $r=a$, and an initial population at $r=r_0$ can be obtained analytically. We denote this solution by $p_0^r(r,t|r_0)$. For $r_0=a$ it reads[18]

$$p_0^r(r,t|a)=(\pi Dt)^{-1/2}\exp[-(r-a)^2/4Dt]\times[1-(\pi Dt)^{1/2}a^{-1}\exp(z^2)\mathrm{erfc}(z)], \tag{21}$$

where $z\equiv(r-a)/\sqrt{4Dt}+\sqrt{Dt}/a$. Setting $r=a$ and taking the first two terms in the asymptotic expansion[19] of the function $\exp(z^2)\mathrm{erfc}(z)$ one finds that

$$p_0^r(a,t|a)\sim(4\pi Dt)^{-3/2}. \tag{22}$$

This result, when inserted in Eq. (20) gives the asymptotic behavior of the survival probability for free diffusion.

The result in Eq. (22) can be extended for the case of a general potential, $V(r)$. Consider the function $q(r,t|r_0)\equiv\exp[-V(r)]p_0^r(r,t|r_0)$. It obeys a reflective boundary condition, $\partial(e^V q)/\partial r=0$ at $r=a$ because p_0^r does so when $V=0$. It is not a solution of Eq. (2) for arbitrary r. However, it is easily seen that $q(r,t|r_0)$ approaches the solution of Eq. (2) for $r\to a$. Hence, $p^r(a,t|r_0)=q(a,t|r_0)$. Therefore one simply needs to multiply Eq. (22) by $\exp[-V(a)]$. Inserting in Eq. (2) one finally has

$$1-Q(t)\sim\frac{\pi a^2\kappa_r\exp[-V(a)]}{2\kappa_d(\pi Dt)^{3/2}}. \tag{23}$$

The special case of an attractive Coulomb potential is obtained by setting $\exp[-V(a)]=\exp(R_D/a)$.

The fact that the asymptotic behavior of the survival probability behaves as $(Dt)^{-3/2}$ could have been guessed from the fact that at long times the recombination reaction is a small perturbation on the diffusive motion.

$$1-Q(t)\sim K_\infty^{-1}(4\pi Dt)^{-3/2}. \tag{23'}$$

The amplitude of a diffusing Gaussian in three dimensions decreases as $(4\pi Dt)^{-3/2}$, while the prefactor is just the equilibrium constant for recombination at infinite dilution, Eq. (19). This result can also be interpreted[9] as dissociation with a rate constant κ_d and an ultimate transient recombination rate which decreases as $t^{-3/2}$.

V. COMPARISON WITH EXPERIMENT

We have seen that the solutions of the rate and diffusion equations are predicted to have completely different asymptotic behavior. We have tried to check whether we could observe the asymptotic behavior experimentally.

The experiments describe in Refs. 8(a) and 9 were repeated, using an extended scale of 4000 ps in the streak-camera apparatus. The pulse width is 20 ps and the width of the streak-camera response function estimated as 11 channels, or 88 ps FWHM. Extra care was taken to eliminate artifacts from the measurement equipment. The theoretical calculations were therefore corrected for 0.6% anion fluorescence "leak" as $0.994(1-Q)+0.006Q$, convoluted with the instrument response function and fitted to the experimental results on a linear scale as before.[8(a)]

The fit is shown in Fig. 5. The relevant parameters are given the legend. The tail of the decay curve is smaller than in our previous measurement,[8(a)] resulting in somewhat different values for κ_r and κ_d. These new values yield $k_{on}=1.0\pm0.2)\times10^{11}\ \mathrm{M^{-1}\,s^{-1}}$, $K_{off}=(5.0\pm0.6)\times10^9\ \mathrm{M^{-1}\,s^{-1}}$, $p\mathrm{K}^*=1.31\pm0.07$. The values obtained from pH titration[20] are $k_{on}=(5\pm0.2)\times10^{10}\mathrm{M^{-1}\,s^{-1}}$, $k_{off}=(2\pm1)\times10^9\ \mathrm{s^{-1}}$ and $p\mathrm{K}^*=1.38\pm0.05$. There is good agreement in the $p\mathrm{K}^*$ values, but the discrepancy in the steady-state rates seems too large to be attributable to errors in the determination of k_d and k_r.

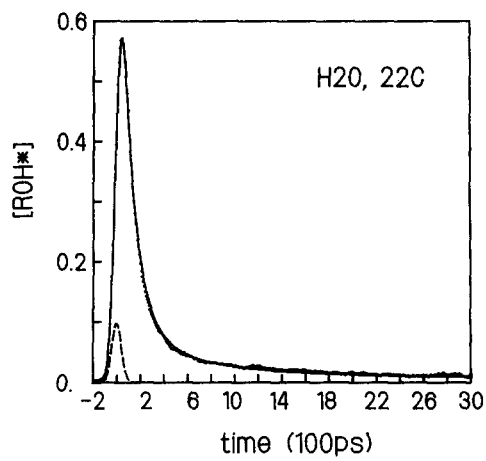

FIG. 5. A fit of the solution (bold curve) of the DSE (2) to the new experimental data (dots) on the decay of HPTS fluorescence by proton transfer. As compared with Ref. 8(a), the present results are taken on the 4000 ps scale of the streak camera (8 ps/channel), with improved signal/noise ratio. The solvent is water, and the temperature 22 °C. The parameters used in the diffusion equation are $D=940$ Å^2/ns, $R_D=28.5$ Å, $a=6.5$ Å, $\kappa_d=10\ \mathrm{ns^{-1}}$, and $\kappa_r=8$ Å/ns. The calculation uses a grid of $\Delta r=0.6$ Å spacing extending to $r_{max}=370$ Å, with time steps of 13 ps. It was multiplied by $\exp(-t/\tau)$ to account for a radiative lifetime of $\tau=6$ ns and corrected for a 0.6% of $\mathrm{RO^-}^*$ fluorescence. Finally, it was convoluted with the laser-pulse/instrument-response function of assumed total width (at half-height) $\sigma=96$ Å, and shifted with respect to the peak in the experimental curve by -8 ps. (A calculation with 2 ps time step was used for an accurate evaluation of these two parameters.)

Results on a log–log scale are shown in Fig. 6. The full curve is the exact numerical solution of Eq. (2). It starts off below the asymptotic line, which is the straight dotted line, crosses it, and converges to it from above. This behavior is expected from the discussion in the previous section: The exact solution is delayed compared to the distribution function for a reflective boundary,[8(c)] resulting in larger density near the boundary and hence more recombination. Therefore, convergence to the asymptotic line is from above.

The dashed curve is the solution of the rate equation (10a). It parallels the exact solution of DSE up to the point where it crosses the asymptotic line. The dashed–dotted line is the result of the approximate model[9] which uses a long-time $t^{-3/2}$ solution for the diffusion-controlled recombination rate. It was fitted to the short-time results.[9] It therefore underestimates the exact results at long times, but approaches the correct asymptotic slope.

The experimental data is shown as dots. It becomes noisy at long times, when less than 1% of the initial population survives. The difference between the models is, however, much larger than the experimental noise, and it is clear that (save for a possible small shift in base line) the data at long times parallels the exact solution of Eq. (2) and not that of the other theories. Even the transition from below to above the asymptotic line is correctly described.

An additional measurement in D_2O, shown in Figs. 7 and 8, tends to support the same conclusion. The parameters are almost the same as in our previous 85 °C measurement.[8(a)] Together with the modified parameters for H_2O we find that the isotopic effect on κ_r is approximately unity, while that on κ_d is about 2.5. This gives $k_{on} = (0.83 \pm 0.2) \times 10^{11}\ M^{-1}\ s^{-1}$, $k_{off} = (1.7 \pm 0.2) \times 10^{9}\ s^{-1}$, and $pK^* = 1.7 \pm 0.1$. As a result, the isotope effect on k_{on}, which is due only to the faster H^+ diffusion, is 1.2. The isotope effect on k_{off} which is 3, is due to the smaller κ_d and D values. ΔpK^* is now 0.4 ± 0.2, in better agreement with values obtained for other molecules in this pK^* range.[21]

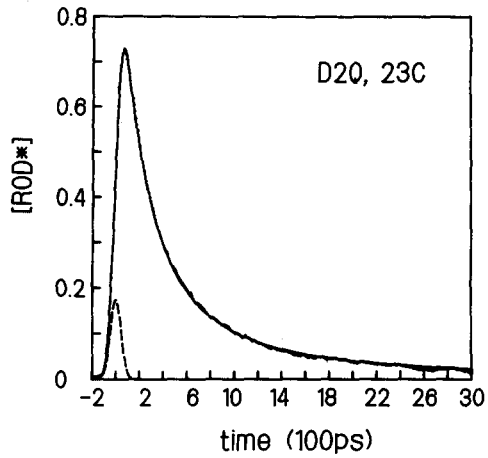

FIG. 7. A fit of the solution (bold curve) of the DSE (2) to the new experimental data (dots) on the excited-state decay of HPTS by proton transfer. The solvent is D_2O, and the temperature 23 °C. The parameters used in the diffusion equation are $D = 650$ Å^2/ns, $R_D = 28.5$ Å, $a = 6.5$ Å, $\kappa_d = 4$ ns^{-1}, and $\kappa_r = 7.8$ Å/ns. The calculation uses a grid of $\Delta r = 0.6$ Å spacing extending to $r_{max} = 300$ Å, with time steps of 15 ps. It was multiplied by $\exp(-t/\tau)$ to account for a radiative lifetime of $\tau = 6$ ns and corrected for a 0.6% of RO^{-*} fluorescence. Finally, it was convoluted with the laser-pulse/instrument-response function of assumed total width (at half-height) $\sigma = 108$ Å.

In order to further investigate the difference between the three theories, we plot in Fig. 9 the time dependent geminate-recombination rates (fluxes). In the range of 0.1–1 ns they are of a similar magnitude, which explains their relative success in fitting the data on a linear scale.

Asymptotically, the recombination rate seems to approach a $t^{-3/2}$ behavior, as expected from Eq. (23) and the approximate model of Ref. 9. Note also that after 3 ns the germinate rate is $\sim 10^8\ s^{-1}$, while the homogeneous rate, ck_{on}, is $3.5 \times 10^5\ s^{-1}$ at $pH = 5.5$. Hence we expect a negligible effect of the homogeneous process on the long-time tail shown in Fig. 6.

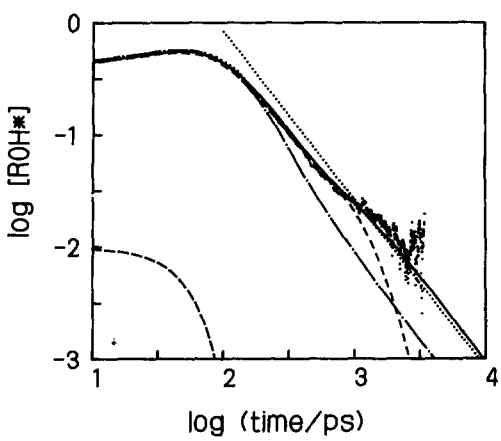

FIG. 6. The data of Fig. 5 on a log–log (base 10) plot. Dots are experimental data, corrected for the radiative lifetime and penetration of the RO^{-*} peak into the ROH^* fluorescence. Bold line is the numerical solution of Eq. (2), convoluted with the instrument response function, which is the downward displaced dashed curve. Straight dotted line is the asymptotic law, Eq. (23), not convoluted. The dashed curve is the bi-exponential solution (10a) for the kinetic scheme (1), with $R_{cc} = 28$ Å. The dash–dotted curve is the approximate solution of Ref. 9. Both curves were convoluted as above.

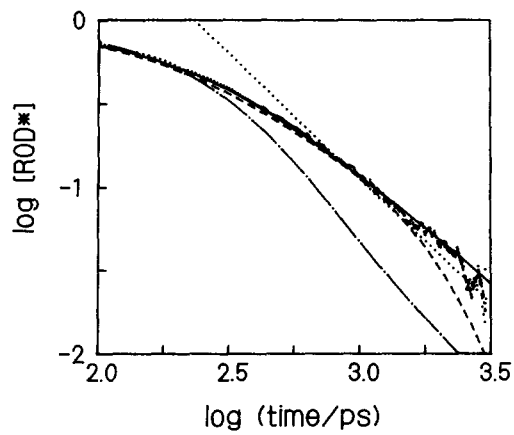

FIG. 8. The data of Fig. 7 on a log–log scale, see legend of Fig. 6. $R_{cc} = 25$ Å.

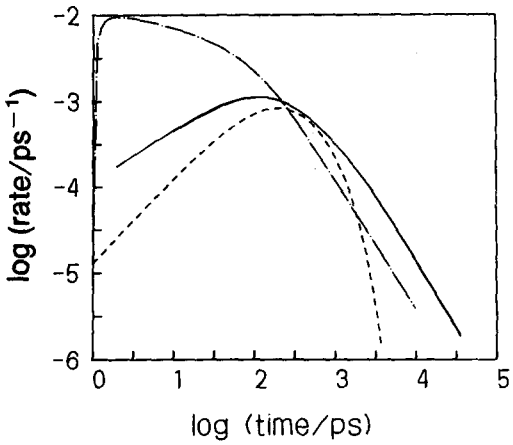

FIG. 9. Recombination reaction rates (in H_2O at 18 °C) for the three models. Bold curve is $4\pi a^2\kappa$, $p(a,t)$, where $p(r,t)$ is the exact numerical solution of the DSE. Dashed curve is $k_2[A\cdots B]$ as obtained from the solution of the kinetic scheme, Eq. (10a). Parameters as in Fig. 3. Dashed–dotted curve is $k_2' t^{-3/2}[A+B]$, according to the approximate model of Ref. 9.

VI. CONCLUSION

We have shown that the exact solution for diffusion with backreaction boundary conditions, which represent a dissociation–recombination process, may be approximated for short times by the bi-exponential solution of the kinetic scheme (1), where a reactive "complex", i.e., an intermediate state between the bound and "free" species, is defined rather formally as the range of distances $a \leqslant r \leqslant R_{cc}$. The conventional presentation[5] has been modified so that steady-state rate coefficients are calculated to and from the "complex cage" radius, R_{cc}. The results suggest that the notion of a complex, or cage, may be physically meaningful at short times. It is defined here for an interparticle potential function $V(r)$ which is completely monotonic in r: Its existence is independent of additional potential barriers along r.[14,15] It therefore has nothing to do with solvent microstructure. It roughly describes the range where the Coulombic attraction is larger than the thermal energy.

The above results may be of practical usefulness in supplying a reasonable analytic approximation to the solution of the diffusion equation: One may first fit experimental results to the analytic solution, extract the relevant parameters from it and use them as the initial guess in the exact solution of Eq. (2).

At long times, when the geminate proton–anion distance distribution becomes very wide, the above conclusions no longer hold. The reaction is then governed mainly by diffusive motion, the intrinsic recombination and dissociation steps being a small pertubation to it. The exact asymptotic behavior is a power law: The concentration of the dissociating molecule decays as $t^{-3/2}$. This can never be mimicked by a kinetic scheme with a finite number of intermediate steps. We have verified this experimentally, as shown in Figs. 6 and 8. Unfortunately, the limitations of the streak-camera detection system do not enable us to obtain reliable results for extremely long times. We hope to achieve this in the future by using a single-photon-counting system.

It also follows from the analysis that when the rate parameters for the bi-exponential kinetic scheme are set to fit the short time transient kinetics, the area under the curve no longer accurately determines the steady-state dissociation rate coefficient k_{off}. This disagreement is expected to become large in situations where the long-time tail has a larger amplitude, such as in solvents of low dielectric constants.

The work described here and in Ref. 8 shows that while the conventional chemical rate equations do not accurately describe picosecond proton dissociation, the Debye–Smoluchowski diffusion equation does so with success. Hence the spatial inhomogeneity in the concentration profiles of chemical species cannot generally be ignored. We believe that future accurate analysis of experimental data for fast chemical reactions will have to rely on the full transient solution of the diffusion equation.

ACKNOWLEDGMENT

D. H. is supported in part by Grant No. 85-00334 from the US–Israel Binational Science Foundation (BSF), Jerusalem, Israel.

APPENDIX A

The association rate coefficient k_2 can itself be broken down to more fundamental steps, for reaction from R_{cc} to contact and from there to the trap, designated by an asterisk. A steady-state assumption gives[15]

$$k_2 = \frac{k(R_{cc}\rightarrow a)k(a\rightarrow *)}{k(a\rightarrow *)+k(a\rightarrow R_{cc})}. \tag{A1}$$

The individual rate constants are again determined from solving Eq. (2′) with absorbing boundary conditions for the final states. Hence

$$4\pi D \exp[V(R_{cc})][k(R_{cc}\rightarrow a)v_{cc}]^{-1} = \int_a^{R_{cc}} \exp[V(r)]r^{-2}\,dr, \tag{A2a}$$

which is Eq. (12c) with $\kappa_r = \infty$ (the volume factor v_{cc} is omitted if Ref. 15), and

$$4\pi D \exp[V(a)]k(a\rightarrow R_{cc})^{-1} = \int_a^{R_{cc}} \exp[V(r)]r^{-2}\,dr. \tag{A2b}$$

The rate constant for trapping at contact is simply

$$k(a\rightarrow *) = 4\pi a^2\kappa_r. \tag{A2c}$$

By inserting Eqs. (A2) into (A1) one rederives Eq. (12c).

APPENDIX B

Here we show that the expression for the ultimate reaction probability (or its complement the ultimate excape probability) from the cage radius R_{cc} is consistent with the above analysis.

The ultimate reaction probability from a distance r, $\eta(r)$, is the solution[17] of the backward equation

$$\frac{d}{dr} Dr^2 e^{-V} \frac{d\eta(r)}{dr} = 0. \tag{B1}$$

A radiation boundary condition at $r = a$ becomes[17]

$$D\frac{d\eta}{dr}\bigg|_{r=a} = \kappa_r \eta(a) . \tag{B2}$$

Comparing these equations to Eq. (2') for the steady-state distribution, $p^{ss}(r)$, and the appropriate boundary condition, Eq. (11c), one observes that[6]

$$\eta(r) = \exp[V(r)]p^{ss}(r) . \tag{B3}$$

The desired solution[17] is

$$\eta(R_{cc}) = \int_{R_{cc}}^{\infty} e^{V(r)} r^{-2}\, dr \Big/ \left[\int_a^{\infty} e^{V(r)} r^{-2}\, dr + De^{V(a)}(a^2\kappa_r)^{-1} \right] . \tag{B4}$$

Comparison with Eqs. (12) and (16) shows that

$$\eta(R_{cc}) = k_2/[k_2 + k_{-D}] = k_{on}/k_D \tag{B5}$$

which is expected result for the kinetic scheme (1). Equation (B5) can be identified with Eq. (30) of Ref. 5, with a replaced by R_{cc}. It can also be written as[5]

$$\eta/\eta^{abs} = k_{on}/k_{on}^{abs} . \tag{B6}$$

The superscript abs denotes an absorbing boundary condition at contact [$\kappa_r = \infty$ in Eqs. (17) and (B4)]. Note that $k_{on}^{abs} = k_D(\infty \to a)$ is just the diffusion rate constant to contact [Eq. (12a) with R_{cc} replaced by a].

APPENDIX C

We show that for one-dimensional free diffusion with backreaction, the asymptotic behavior is identical to that obtained by the procedure of Sec. IV. The analytic solution is obtained, as in Ref. 7(c), by the Laplace transform method. The difference is that here the initial population is concentrated in the trap.

Using the Laplace transform for the probability density

$$\bar{p}(x,s) \equiv \int_0^{\infty} p(x,t) \exp(-st)dt , \tag{C1}$$

together with the initial conditions $p(x,0) = 0$, the one-dimensional (x-coordinate) diffusion equation for the case $V(x) = 0$ reads

$$s\bar{p}(x,s) = D\frac{\partial^2 \bar{p}}{\partial x^2} , \tag{C2}$$

with $\bar{p}(x,\infty) = 0$. Using

$$Q(t) = -D\int_0^t \frac{\partial p(x,t')}{\partial x}\bigg|_{x=0} dt' \tag{C3}$$

the boundary condition at $x = 0$ becomes

$$\kappa_d + (s+\kappa_d)D\frac{\partial \bar{p}}{\partial x}\bigg|_{x=0} = s\kappa_r \bar{p}(0,s) . \tag{C4}$$

The solution to Eq. (C2),

$$\bar{p}(x,s) = A(s)\exp(-\sqrt{s/D}\, x) , \tag{C5}$$

is inserted into Eq. (C4) to determine $A(s)$,

$$A(s) = \kappa_d (D\sqrt{sD}\,\Delta)^{-1} \times \left\{ [\sqrt{s/D} + (\kappa_r - \Delta)/2D]^{-1} - [\sqrt{s/D} + (\kappa_r + \Delta)/2D]^{-1} \right\} , \tag{C6}$$

where $\Delta \equiv (\kappa_r^2 - 4D\kappa_d)^{1/2}$. Inversion of the Laplace transform gives

$$p(x,t) = \kappa_d \Delta^{-1} \exp(-x^2/4Dt) \times [\exp(z_-^2)\operatorname{erfc}(z_-) - \exp(z_+^2)\operatorname{erfc}(z_+)] , \tag{C7}$$

where $z_{\pm} \equiv [x + (\kappa_r \pm \Delta)Dt]/\sqrt{4Dt}$.

The survival probability can now be obtained directly from Eq. (3),

$$\Delta[1 - Q(t)] = \tfrac{1}{2}(\kappa_r + \Delta)\exp[(\kappa_r - \Delta)^2 Dt/4] \times \operatorname{erfc}[(\kappa_r - \Delta)\sqrt{Dt}/2] - \tfrac{1}{2}(\kappa_r - \Delta) \times \exp[(\kappa_r + \Delta)^2 Dt/4]\operatorname{erfc}[(\kappa_r + \Delta)\sqrt{Dt}/2] . \tag{C8}$$

The limiting behavior is easily determined by taking the first term in the asymptotic expansion[19] $\exp(z^2)\operatorname{erfc}(z) \sim 1/\sqrt{\pi}z$. This gives

$$1 - Q(t) \sim \frac{\kappa_r}{\kappa_d\sqrt{\pi Dt}} . \tag{C9}$$

On the other hand, the method of Sec. IV gives

$$1 - Q(t) \sim \frac{\kappa_r}{\kappa_d} p^r(0,t\,|0) , \tag{C10}$$

where $p^r(x,t\,|0)$ is the solution of the same problem but with a reflecting boundary condition at $x = 0$ and an initial delta function located there. This solution is easily obtained

$$p^r(x,t\,|0) = (\pi Dt)^{-1/2}\exp(-x^2/4Dt) . \tag{C11}$$

Indeed, inserting it into Eq. (C10) leads to the asymptotic behavior, Eq. (C9), as derived from the exact analytic solution.

[1] M. von Smoluchowski, Ann. Phys. **48**, 1103 (1915).
[2] P. Debye, Trans. Electrochem. Soc. **82**, 265 (1942).
[3] F. C. Collins and G. E. Kimball, J. Colloid. Sci. **4**, 425 (1949).
[4] M. Eigen, Z. Phys. Chem. **1**, 176 (1956).
[5] D. Shoup and A. Szabo, Biophys. J. **40**, 33 (1982).
[6] U. M. Gösele, Prog. React. Kinet. **13**, 65 (1984).
[7] (a) F. C. Goodrich, J. Chem. Phys. **22**, 588 (1954); (b) D. L. Weaver, *ibid.* **72**, 3483 (1980); (c) N. Agmon, *ibid.* **81**, 2811 (1984).
[8] (a) E. Pines, D. Huppert, and N. Agmon, J. Chem. Phys. **88**, 5620 (1988); (b) N. Agmon, *ibid.* **88**, 5639 (1988); (c) submitted for publication.
[9] E. Pines and D. Huppert, Chem. Phys. Lett. **126**, 88 (1986); J. Chem. Phys. **84**, 3576 (1986).
[10] G. G. Hammes, *Principles of Chemical Kinetics* (Academic, New York, 1978), p. 66.
[11] N. Bjerrum, Kgl. Danske Vidensk. Selsk. **7**, No. 9 (1926).
[12] R. M. Fuoss, J. Am. Chem. Soc. **80**, 5059 (1958).
[13] M. Hauser, H.-P. Haar and U. K. A. Klein, Ber. Bunsenges. Phys. Chem. **81**, 27 (1977).
[14] C. A. Emeis and P. L. Fehder, J. Am. Chem. Soc. **92**, 2246 (1970); P. L. Fehder, C. A. Emeis, and R. P. Futrelle, J. Chem. Phys. **54**, 4921 (1971).
[15] S. H. Northrup and J. T. Hynes, J. Chem. Phys. **71**, 871, 884 (1979).
[16] P. Pechukas, Annu. Rev. Phys. Chem. **32**, 159 (1981), and references therein.
[17] H. Sano and M. Tachiya, J. Chem. Phys. **71**, 1276 (1979).
[18] H. S. Carslaw and J. C. Jaeger, *Conduction of Heat in Solids*, 2nd ed. (Clarendon, Oxford, 1959), Eq. (14.7.16).
[19] M. Abramowitz and I. A. Stegun, *Handbook of Mathematical Functions* (Dover, New York, 1965), Eq. (7.1.23).
[20] A. Weller, Z. Phys. Chem. N.F. **17**, 242 (1958).
[21] E. L. Wehry and L. B. Rogers, J. Am. Chem. Soc. **88**, 351 (1966).